13

Determination of the activation energy of the disproportionation reaction of amorphous GeO_x film on quartz substrate using Raman spectroscopy

© Fan Zhang,[1] M. Vergnat,[2] V.A. Volodin[1,3]

[1] Novosibirsk State University, Novosibirsk, Russia
[2] Universite de Lorraine, CNRS, IJL, Nancy, France
[3] Rzhanov Institute of Semiconductor Physics, Siberian Branch, Russian Academy of Sciences, Novosibirsk, Russia; Novosibirsk State University, Novosibirsk, Russia
e-mail: volodin@isp.nsc.ru

Received April 6, 2023
Revised May 15, 2023
Accepted May 15, 2023

Amorphous germanium nanoclusters were formed in the GeOx film on quartz as a result of the disproportionation reaction GeO_x during furnace annealing. To determine the reaction activation energy, annealing was carried out at temperatures from 400 to 500°C. The appearance and growth of amorphous germanium nanoclusters were investigated using Raman spectroscopy. It was found that the position of the Raman scattering peak from amorphous germanium varied with the annealing time, which due to the change in the sizes of nanoclusters, i.e., the phonon localization model can be applied not only to germanium nanocrystals, but also to amorphous germanium clusters, in the case of their ultra-small sizes. In addition, it was found that the saturation time for the formation of amorphous germanium nanoclusters depends exponentially on the annealing temperature. The kinetics analysis of the nanocluster's formation was carried out within the framework of the Johnson-Mehl-Avrami-Kolmogorov model. The activation energy of the disproportionation reaction was obtained for the first time, which amounted to 1.0 ± 0.1 eV.

Keywords: germanium oxide, disproportionation reaction, JMAK model, activation energy.

DOI: 10.61011/TP.2023.08.57275.74-23

Introduction

In recent years, there is interest in silicon or germanium oxide films containing amorphous nanoclusters or nanocrystals (NCs) of silicon or germanium, due to the fact that the nanoparticles in the dielectric matrix are quantum dots [1,2]. Using quantum-size effects, it is possible to control the optical properties of Ge clusters [3], i.e., such clusters are capable of emitting light in the near-IR and visible ranges [4,5]. Besides, germanium oxide films (GeO_x) can be used in electronics. Germanium oxide has high transparency in the visible and near-IR ranges, as well as a relatively high refractive index. These properties allow the use of GeO_x films in various devices, such as LEDs [6,7], solar cells [8,9] and transistors [10]. Besides, thin layers GeO_x are used in germanium-based MOS structures as surface passivation layers due to the low density of interface states [11]. However, the production of Ge-based MIS transistors has some challenges, such as higher leakage current, high density of surface states, and thermal stability problems, which need to be addressed for their wider use in commercial applications [12–14].

Quartz is one of the most stable materials used in electronics and is therefore often used as a substrate for the creation of electronic and optoelectronic components. GeO_x films can be used as a coating on quartz glasses to change their optical properties, such as light transmission and reflection. This could be especially useful in the production of solar cells or optical devices. Thus, GeO_x films on quartz substrate have a wide range of applications in various fields such as microelectronics, nanotechnology and optical devices.

It is worth noting that GeO_x films are more chemically stable than GeO_2 [15] films, however, amorphous GeO_x films are thermally metastable. As the temperature increases in amorphous films GeO_x, the disproportionation reaction of $GeO_x \rightarrow \left(1 - \frac{x}{2}\right)Ge + \frac{x}{2}GeO_2$ occurs [16,17]. In the case of GeO films during complete disproportionation the reaction $2GeO \rightarrow Ge + GeO_2$ occurs [18]. Furnace annealing is widely used to form amorphous germanium nanoclusters and their crystallization in films of amorphous nonstoichiometric germanium oxide. For example, furnace annealing at a temperature of 550°C, 30 min, led to the formation of amorphous germanium clusters and their partial crystallization [19]. At the same time, to date, only two papers are known relating study of the kinetics of the formation of germanium nanoclusters in GeO films and determination of the activation energy of the disproportionation reaction [20,21]. It is worth noting that the influence of the stoichiometric composition (parameter x) of GeO_x films on the kinetics of the disproportionation reaction was not previously studied at all.

In this paper we studied for the first time the temperature effect on the kinetics of the formation of amorphous germanium nanoclusters and determined the activation energy of the disproportionation reaction for the amorphous

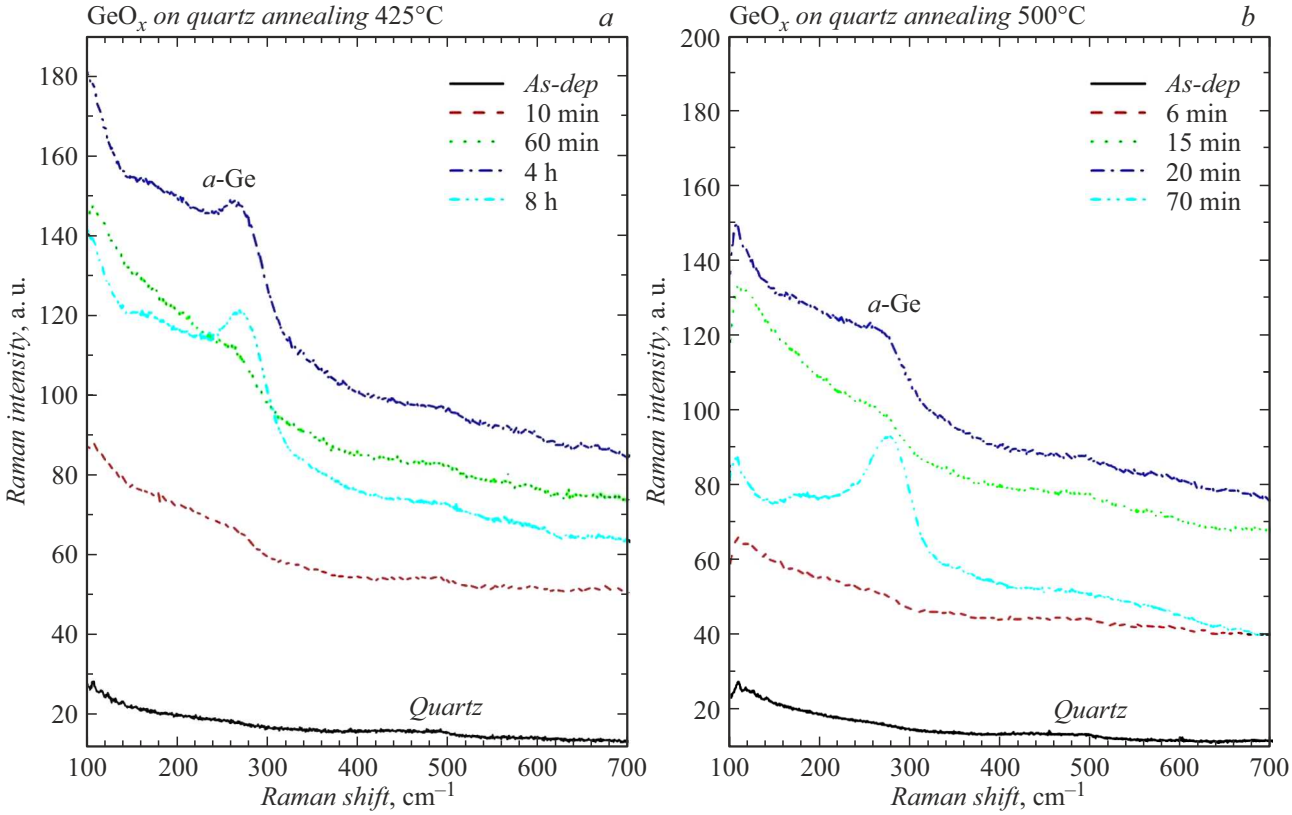

Figure 1. Raman spectra of the film GeO_x during annealing: *a* — 425, *b* — 500°C.

film GeO_x ($x \sim 1.1$) on quartz substrate. It was also discovered for the first time that the Raman spectra of amorphous germanium nanoclusters depend on their sizes, i.e. the phonon localization model can be used not only for germanium nanoclusters [22], but also for amorphous germanium nanoclusters in the case of their ultra-small sizes.

1. Experiment description

One of the ways to create films GeO_x with a stoichiometric parameter x, which is ~ 1.1, is the method of electron beam sputtering in a vacuum. This method makes it possible to obtain films on quartz substrate. The method is based on the use of a beam of electrons that bombard a target (powders GeO_2) located in a vacuum chamber (the pressure in the reactor was 10^{-6} Pa). In this case, the target material is sputtered and deposited on the surface of the cold substrate. In our case, the film was coated with a protective layer SiO_2, obtained directly in the same reactor, in order to avoid evaporation of germanium monoxide during post-growth annealing [23]. A series of annealings were carried out using MILA-5000-UHV furnace heated with incandescent lamps at atmospheric pressure in an air atmosphere. Annealing temperatures ranged from 400 to 500°C, temperature maintenance accuracy was ±0.1°C.

Raman spectroscopy was used to analyze the film structure. Raman spectra were measured on T64000 Horiba Yobin Yvon spectrometer in backscattering geometry. The spectral resolution was $\sim 2\,\mathrm{cm}^{-1}$. To excite Raman radiation a GFL-515-0200-FS fiber laser line (Inversiya-Fiber, Novosibirsk, Russia) with a wavelength of 514.5 nm was used. The laser radiation spot on the sample was of size $\sim 10\,\mu$m, its power was approximately 1 mW, which did not cause noticeable heating of the samples.

2. Results and discussion

According to the available literature data, it can be stated that temperature greatly affects the rate of the disproportionation process [24], therefore, in this paper, annealing was carried out at various temperatures — from 400 to 500°C to study the kinetics of the formation of amorphous germanium nanoclusters.

Figure 1 shows the Raman spectra of GeO_x film deposited on quartz substrate after annealing at temperatures of 425 and 500°C depending on the annealing time. As can be seen, in the Raman spectra of the initial film there are no signals from amorphous germanium clusters; one can only observe the features arising from scattering on the quartz substrate, — this is a wide band and a small peak at $\sim 495\,\mathrm{cm}^{-1}$. Perhaps this feature is explained by oscillations of the Si–Si bonds in defect complexes [25]. The signal

from the quartz substrate is observed because GeO_x film is translucent to laser radiation with wavelength of 514.5 nm. So, we can say that there are no nanoparticles (amorphous or crystalline germanium clusters) in the original film, at least in an amount sufficient for their detection by Raman spectroscopy.

It is known that germanium NCs contribute to the Raman spectrum in the form of a relatively narrow peak, the position of which ranges from 290 to 300 cm $^{-1}$ and depends on the size of the NCs [25]. As the NC sizes increase, the position of the Raman peak from them shall shift towards the peak from single-crystalline germanium, which is 301.5 cm $^{-1}$ [26]. Due to the fact that amorphous germanium has no periodic structure, which leads to a lack of translational symmetry, the law of conservation of quasi-momentum is not satisfied when light is scattered in it. The Raman spectrum of amorphous substances reflects the effective density of their vibrational states. In the Raman spectrum of amorphous germanium, a wide band appears with a maximum at approximately 275 cm $^{-1}$ [27]. As can be seen from Fig. 1, after annealing this band appears in the Raman spectra, i.e., annealing led to the formation of amorphous germanium clusters in the film. In this case, at the annealing temperature 425°C, the time for the formation of amorphous germanium clusters is 10 min (600 s), but at the temperature 500°C this time is 6 min (360 s). During further annealing one can see how the peak from amorphous germanium increased. Obviously, this was due to the growth of amorphous germanium nanoclusters. However, over time the process of formation of these nanoclusters becomes saturated, which is associated with decrease in the content of excess germanium in the matrix surrounding the germanium nanoclusters. The saturation time for the formation of amorphous germanium clusters in the film during annealing at temperature 425°C is approximately 8 h, and during annealing at temperature 500°C — approximately 70 min. This means that the higher the annealing temperature is, the faster the formation of germanium nanoclusters is.

The Raman spectra were analyzed using the Fityk program. The background was removed from the spectra (by subtracting a straight line in the range from 150 to 300 cm^{-1}), and then the spectra were deconvoluted into Gaussian curves, and the positions and intensities of the Raman peaks were found. It is known that the Raman spectrum of amorphous inclusions is asymmetrical; it simply reflects the effective density of vibrational states of Ge−Ge bonds. Asymmetry was taken into account in the following way: the spectra were approximated by two Gaussian curves (with different linewidth), the sum of the two curves quite adequately described the shape of the spectrum. The position of the narrow and more intense Gaussian curve was taken as the position of the Raman peak; the sum of the areas of both Gaussian curves was taken as the integral intensity of the Raman band from amorphous germanium clusters. All these data were obtained for all temperatures and for all annealing times. As an example Fig. 2 shows the

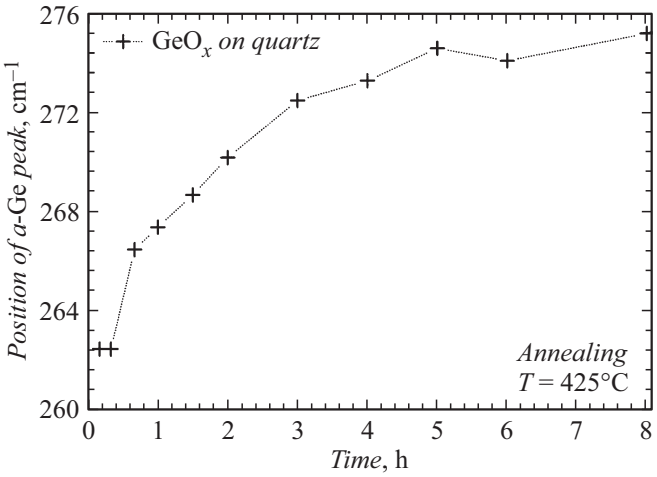

Figure 2. POSITION of Raman peaks vs. annealing time at temperature 425°C.

Raman peak position vs. annealing time at the temperature 425°C. The Figure shows that after annealing for 10 min, the position of the Raman peak from amorphous germanium nanoclusters was not 275 cm^{-1} (as should be in the case of continuous film of amorphous germanium), but 262 cm^{-1}. Apparently, at the initial stage of formation the size of amorphous germanium nanoclusters in our case is less than 1 nm, this size is less than the phonon correlation length in amorphous germanium. It is known that it is small, and is estimated to be 1.2−1.5 nm [28]. Note that with annealing time increasing, the position of the peak from amorphous germanium shifts towards higher frequencies — up to 275 cm^{-1}; apparently, this is due to the increase in their size during the annealing process. By analyzing the dependence of the Raman peak position on the annealing time, it is possible to more accurately determine the saturation time of the formation of amorphous germanium clusters during the annealing process. From Fig. 2 it is clear that the positions of the Raman peaks practically did not change after annealing for 5 h or more, thus, it can be stated that at temperature 425°C the saturation time is approximately 5;h (18 000 s).

In translucent films, the integral intensity of the Raman signal (it is proportional to the product of the height of the Raman peak and its width) will be proportional to the number of bonds Ge−Ge, i.e., the volume fraction of germanium nanoclusters, therefore to describe the kinetics of the formation of amorphous germanium nanoclusters, one can use the dependence of the integral intensity of the Raman peak of amorphous germanium nanoclusters on the annealing time (Fig. 3). To improve the accuracy of determining the integral intensity of the Raman peak from amorphous germanium nanoclusters, the Raman signal was each time compared with the signal from a reference sample-a single crystal silicon wafer. This made it possible to avoid possible errors associated with power fluctuations of the exciting laser and the accuracy of adjustment when

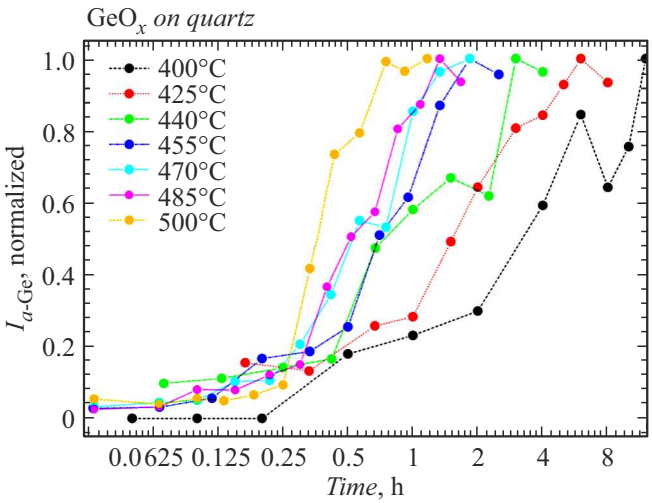

Figure 3. Normalized intensity of Raman peak from amorphous germanium clusters vs. annealing time for annealing temperatures from 400 to 500°C (7 temperatures in total). For easy perception, the annealing time is given on a logarithmic scale.

recording Raman spectra. Fig. 3 shows the normalized intensities of the Raman peak from amorphous germanium clusters depending on the annealing time at all annealing temperatures used. From the spectrum deconvolution into peaks (Gaussian curves), their integral intensities were obtained, and then they were normalized by dividing by the value of the most intense peak after annealing at each temperature. Thus, as can be seen from Fig. 3, the normalized intensity could not exceed unity. Note that with increase in the annealing temperature from 400 to 500°C, the saturation time for the formation of amorphous germanium clusters in the film during the annealing process decreases from 8 to approximately 1 h.

Let us proceed to the analysis of the kinetics of the formation of amorphous germanium nanoclusters. Let us introduce the parameter y — the degree of completion of the disproportionation reaction: $y = 0$ if the reaction did not yet begin, and $y = 1$ if the reaction completed (saturation of the formation of amorphous germanium nanoclusters occurred). Then, depending on this parameter, the film composition will be as follows: $(1-y)2\mathrm{GeO}_x + y\left(x\mathrm{GeO}_2 + (2-x)\mathrm{Ge}\right)$. It is obvious that the volume fraction of amorphous germanium nanoclusters is proportional to the parameter y, i.e., by examining the normalized intensity of the Raman peak from amorphous germanium clusters depending on the annealing time (data in Fig. 3), the kinetics of the disproportionation reaction can be analyzed. For the growth of germanium nanoclusters it is necessary to have „excess“ germanium in the surrounding matrix. If we assume that the reaction rate is determined only by the amount of „excess“ germanium in the matrix, we obtain the following differential equation:

$$\frac{\partial y}{\partial t} = \frac{(1-y)}{\tau}, \qquad (1)$$

Conditions for diffusion-controlled growth

Particles of all shapes, growing from small sizes, at nucleation rate:	n
Increasing	$> 5/2$
Constant	5/2
Decreasing	3/2–5/2
Zero	3/2
Growth of particles of noticeable initial volume	1–3/2

where τ — a parameter that has the dimension of time, it includes the diffusion coefficient and the probability of germanium atom incorporation into nanoclusters. Both the diffusion coefficient and the probability of incorporation depend on temperature. From the initial conditions $y(0) = 0$ the solution to equation (1) is

$$y(t) = 1 - e^{-t/\tau}. \qquad (2)$$

In general, the reaction rate is determined by the shape of the growing nanoparticles [24,29] (for example, needles, plates or cylinders), as well as the rate of nucleation [24]. In our case, based on previously obtained electron microscopy data, amorphous germanium clusters have a shape close to spherical [3], and the main kinetic factor is not the shape, but the rate of nanoparticle nucleation. Then, depending on whether the nucleation rate increases, decreases, or remains constant, the degree n appears in equation (2). So, the so-called Kolmogorov–Johnson–Mehl–Avrami equation appears (eng. Kolmogorov–Johnson–Mehl–Avrami equation, JMAK) [30]:

$$y(t) = 1 - e^{-(t/\tau)^n}. \qquad (3)$$

This equation describes the process of formation of amorphous germanium nanoclusters during the disproportionation reaction. In this case, to describe the experimental data shown in Fig. 3, it is necessary to adjust two parameters — τ and n, where τ — this is the time of the knee point of the second derivative of the function $y(t)$ in equation (3) (as already noted, this parameter depends on the annealing temperature and the activation energy of the disproportionation reaction), n — Avrami kinetic index of the disproportionation reaction (as already noted, it depends on the shape of the particles, as well as on the rate of their nucleation). Using the Origin program, we carried out a procedure for approximating the kinetics calculated using formula (3) to the experimentally observed kinetics and determined the parameters τ and n for all temperatures. As an example, Fig. 4 shows the adjustment results for two temperatures.

It can be seen that at the annealing temperature 440°C the best agreement between the experimental kinetics and the theory is observed if the degree n is equal to unity, however, at the annealing temperature 470°C the best

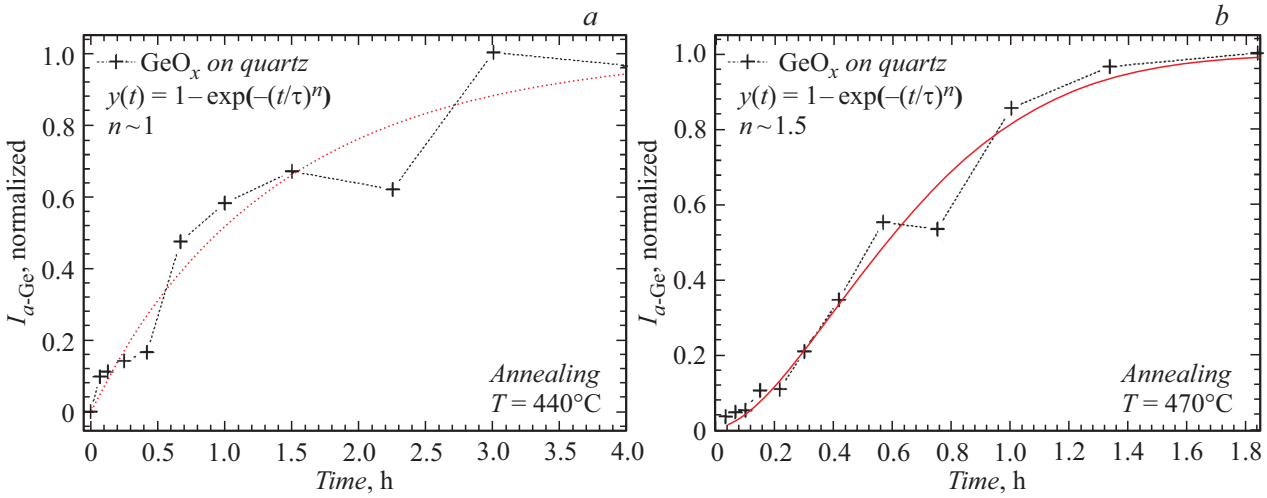

Figure 4. Experimental dependence of the normalized intensity of the Raman peak from amorphous germanium clusters on the annealing time in comparison with the kinetics determined by formula (3) for annealing temperatures: *a* — 440, *b* — 470°C.

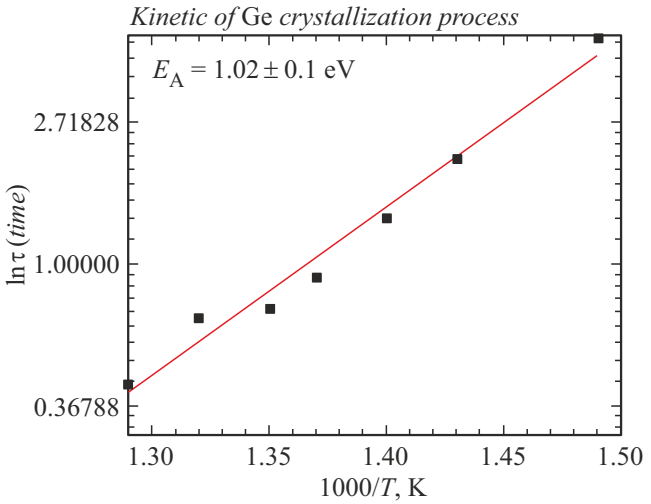

Figure 5. Graph of the natural logarithm of the parameter τ vs. inverse temperature.

agreement was obtained at the degree n equal to 1.5. According to the Table, the value of the degree n lies in the range from 1 to 1.5 in the case of growth of particles with a noticeable initial volume, which is observed at low annealing temperatures — from 400 to 470°C. During annealing 500°C, with the best agreement between the experiment and the theoretical dependence (3), the value of the degree n increased to 2. This means that the rate of nucleation of new germanium clusters decreases, since the kinetics of the nucleation process also has an activation nature of dependence on temperature. Note that determining the kinetics of nucleation of germanium clusters is separate problem. To determine the activation energy (temperature) of nucleation, it is necessary to study in detail the kinetics of the formation of amorphous germanium nanoclusters at the initial stage of the disproportionation reaction (for $y \leq 0.1$).

Fig. 5 shows a graph of the natural logarithm of the parameter τ depending on the inverse temperature. As already noted, the parameter τ includes the temperature dependence of the diffusion coefficient and the atom incorporation into nanocluster, which can be described by the Arrhenius dependence, as in the paper [31]:

$$\tau = Ce^{T_a/T}. \tag{4}$$

Taking the logarithm of the equation (4), we obtain

$$\ln\tau = \frac{T_a}{T} + \mathrm{A}, \tag{5}$$

where T_a — activation temperature, T — annealing temperature and A — constant equal to $\ln(C)$. The relationship for converting activation temperature to activation energy (in electronvolts) is $E_a = T_a/11598$ [eV]. So, from the slope of the approximating straight line, the activation energy of the disproportionation reaction GeO_x was obtained, which amounted to 1.0 ± 0.1 eV.

Conclusion

So, for the first time in GeO_x film on the quartz substrate, it was discovered that the phonon localization model can be applied not only to germanium nanocrystals, but also to amorphous germanium clusters in the case of their ultrasmall sizes, presumably less than 1 nm, — smaller than the phonon correlation length in amorphous germanium. Besides, it was found that the Avrami kinetic exponent n increases with annealing temperature increasing, and the saturation time for the formation of amorphous germanium clusters depends on the annealing temperature. With increasing annealing temperature n increases from 1 to 2, and the saturation time for the formation of amorphous germanium clusters decreases from 5 to 1 h (from 18 000 to 3600 s). The activation energy of the disproportionation

reaction for the amorphous film GeO_x on quartz substrate is calculated to be 1.0 ± 0.1 eV.

Acknowledgments

The authors are grateful to the Center for Collective Use „VTAN“ Novosibirsk State University, for providing the equipment for recording Raman spectra.

Funding

The study was carried out within the framework of the state assignment of the Ministry of Science and Higher Education of the Russian Federation (topic № FWGW-2022-0011 Physical phenomena in quantum structures for components of nanoelectronics, nanophotonics and spintronics).

Conflict of interest

The authors declare that they have no conflict of interest.

References

[1] Z. Ni, S. Zhou, S. Zhao, W. Peng, D. Yang, X. Pi. Mater. Sci. Engineer.: R: Reports, **138**, 85 (2019). DOI: 10.1016/j.mser.2019.06.001
[2] P.-Y. Hong, C.-H. Lin, I.-H. Wang, Y.-J. Chiu, B.-J. Lee, J.-C. Kao, C.-H. Huang, H.-C. Lin, T. George, P.-W. Li. Appl. Phys. A, **129**, (2023). DOI: 10.1007/s00339-022-06332-z
[3] M.P. Gambaryan, G.K. Krivyakin, S.G. Cherkova, M. Stoffel, H. Rinnaert, M. Vergnat, V.A. Volodin. FTT **62**, 434 (2020) (in Russian). DOI: 10.21883/ftt.2020.03.49010.600
[4] N. Shirahata. J. Solid State Chem., **214**, 74 (2014). DOI: 10.1016/j.jssc.2013.10.021
[5] S. Takeoka, M. Fujii, S. Hayashi, K. Yamamoto. Phys. Rev. B, **58**, 7921 (1998). DOI: 10.1103/PhysRevB.58.7921
[6] D. Marris-Morini, V. Vakarin, J.M. Ramirez, Q. Liu, A. Ballabio, J. Frigerio, M. Montesinos, C. Alonso-Ramos, X. Le Roux, S. Serna, D. Benedikovic, D. Chrastina, L. Vivien, G. Isella. Nanophotonics, **7**, 1781 (2018). DOI: 10.1515/nanoph-2018-0113
[7] V. Reboud, A. Gassenq, J.M. Hartmann, J. Widiez, L. Virot, J. Aubin, K. Guilloy, S. Tardif, J.M. Fédéli, N. Pauc, A. Chelnokov, V. Calvo. Progress in Crystal Growth and Characterization Mater., **63**, 1 (2017). DOI: 10.1016/j.pcrysgrow.2017.04.004
[8] D. Lv, M.L. Gordin, R. Yi, T. Xu, J. Song, Y.-B. Jiang, D. Choi, D. Wang. Advanced Functional Mater., **24**, 1059 (2013). DOI: 10.1002/adfm.201301882
[9] J. Zhang, T. Yu, J. Chen, H. Liu, D. Su, Z. Tang, J. Xie, L. Chen, A. Yuan, Q. Kong. Ceramics Intern., **44**, 1127 (2018). DOI: 10.1016/j.ceramint.2017.10.069
[10] Y. Xu, G. Han, H. Liu, Y. Wang, Y. Liu, J. Ao, Y. Hao. Nanoscale Research Lett., **14**, Art. Num. 126 (2019). DOI: 10.1186/s11671-019-2958-2
[11] M. Ke, M. Takenaka, S. Takagi. ACS Appl. Electron. Mater., **1**, 311 (2019). DOI: 10.1021/acsaelm.8b00071
[12] Q. Looker, M. Amman, K. Vetter. Nuclear Instrum. Methods in Phys. Research Section A: Accelerators, Spectrometers, Detectors and Associated Equipment. **777**, 138 (2015). DOI: 10.1016/j.nima.2014.12.104
[13] Y. Li, H. Guo, Y. Yao, P. Dutta, M. Rathi, N. Zheng, Y. Gao, S. Sun, J.-H. Ryou, P. Ahrenkiel, V. Selvamanickam. Cryst. Eng. Comm., **20**, 6573 (2018). DOI: 10.1039/c8ce01258j
[14] D. Lei, K.H. Lee, S. Bao, W. Wang, S. Masudy-Panah, C.S. Tan, E.S. Tok, X. Gong, Y.-C. Yeo. Appl. Phys. Lett., **111**, 252103 (2017). DOI: 10.1063/1.5006994
[15] J. Zhao, L. Yang, J.A. McLeod, L. Liu. Scientific Reports, **5**, Art. Num. 17779 (2015). DOI: 10.1038/srep17779
[16] M. Ardyanian, H. Rinnert, X. Devaux, M. Vergnat. Appl. Phys. Lett., **89**, 011902 (2006). DOI: 10.1063/1.2218830
[17] S. Kai Wang, H.-G. Liu, A. Toriumi. Appl. Phys. Lett., **101**, 061907 (2012). DOI: 10.1063/1.4738892
[18] V.A. Volodin, E.B. Gorokhov. *Quantum Dots: Research, Technology and Applications* (Nova Science Publishers Inc., NY., 2008), p. 333−372.
[19] F. Zhang, V.A. Volodin, K.N. Astankova, G.N. Kamaev, I.A. Azarov, I.P. Prosvirin, M. Vergnat. Results in Chem., **4**, 100461 (2022). DOI: 10.1016/j.rechem.2022.100461
[20] S. Rath, D. Kabiraj, D.K. Avasthi, A. Tripathi, K.P. Jain, M. Kumar, H.S. Mavi, A.K. Shukla. Nucl. Instrum. Methods in Phys. Res. Section B: Beam Interactions with Materials and Atoms, **263**, 419 (2007). DOI: 10.1016/j.nimb.2007.07.018
[21] EB Gorokhov, V.V. Grischenko. *Ellipsometriya: teoriya, metody primeneniya* (Nauka, Novosibirsk, SO RAN, 1987), s. 147 −151. (in Russian)
[22] V.A. Volodin, D.V. Marin, V.A. Sachkov, E.B. Gorokhov, H. Rinnert, M. Vergnat. J. Experiment. Theor. Phys., **118**, 65 (2014). DOI: 10.1134/s1063776114010208
[23] S.R.M. da Silva, G.K. Rolim, G.V. Soares, I.J.R. Baumvol, C. Krug, L. Miotti, F.L. Freire, M.E.H.M. da Costa, C. Radtke. Appl. Phys. Lett., **100**, 191907 (2012). DOI: 10.1063/1.4712619
[24] O.V. Abramov, Ch.V. Kopetsky, A.V. Serebryakov (ed.). *Fizicheskoe metallovedenie* (per. s angl. Metallurgiya, M., 1987) (in Russian)
[25] V.A. Volodin, V.A. Gritsenko, A. Chin. Pisma v ZHTF, **44** 37 (2018) (in Russian). DOI: 10.21883/pjtf.2018.10.46097.17223
[26] J.H. Parker, D.W. Feldman, M. Ashkin. Phys. Rev., **155**, 712 (1967). DOI: 10.1103/physrev.155.712
[27] M. Wihl, M. Cardona, J. Tauc. J. Non-Crystalline Solids, **8**–**10**, 172 (1972). DOI: 10.1016/0022-3093(72)90132-9
[28] M.H. Brodsky. V sb. *Light Scattering in Solids, ser. Topics in Applied Physics,* 205 (1975). DOI: 10.1007/978-3-540-37568-5_5
[29] V.V. Koryakina, E.Yu. Shits. Condensed Matter and Interphases, **22** (3), 327 (2020). DOI: 10.17308/kcmf.2020.22/2963
[30] A.N. Kolmogorov. Bull Acad. Sci. URSS, **3**, 355 (1937).
[31] C.J. Meechan, J.A. Brinkman. Phys. Rev., **103**, 1193 (1956).

Translated by I.Mazurov